

A Multifunctional Hybrid Hip Joint for Improved Adaptability in Miniature Climbing Robots

Satya P. Krosuri and Mark A. Minor
Department of Mechanical Engineering
University of Utah
Salt Lake City, UT 84112, U.S.A
Email: minor@mech.utah.edu

Abstract - The subject of this paper is a hybrid hip biped climbing robot. The hybrid hip provides both prismatic and revolute motion, discretely, to the robot, using a single actuator. This is intended to improve its adaptability in confined environments and its capability to maneuver over and around obstacles. Optimization of the hybrid hip relative to robot size, weight, and actuation limits is considered while maximizing range of motion. The mechanical structure of the robot is discussed, as well as forward and inverse kinematics for motion planning. Workspace analysis indicates that the hip provides an appreciable improvement in foot placement capability when compared to a purely prismatic or revolute hip movement.

1. INTRODUCTION

The subject of this paper is a new type of kinematic structure for climbing robots based upon a hybrid hip joint capable of performing multiple functions with a single actuator. Namely, the hip of the biped can operate as either a prismatic joint or revolute joint, discretely, depending on joint position, Figure 1. As each of these types of joints has its own specialization, the intended purpose of the hybrid joint is to provide increased adaptability and functionality by allowing both of these types of motion. Similar to a prismatic joint, the robot should operate well in confined environments, and similar to the revolute joint the robot should perform well while crossing between surfaces with a wide range of relative inclinations. The subject of this paper is the optimal design, kinematics, and resulting workspace of a hybrid hip climbing robot.

In Section 2, we examine existing climbing robots in the literature and compare the hybrid hip to several of the most similar systems. The mechanical design of the hybrid hip robot is explained in Section 3, and its optimization is considered in Section 4 with a special emphasis on range of motion, force minimization, and small robot size. Section 5 describes the kinematics of this unique structure and Section 6 studies the resulting workspace of the system while in each of the discrete hybrid modes and examines the cumulative affect of the joint. Concluding remarks and future work are presented in Section 7.

2. BACKGROUND

Most climbing robots in the literature are intended for maintenance or inspection in environments such as the exterior of buildings, storage tanks, nuclear facilities, or surveillance and reconnaissance within buildings [1], [2]. Thus, numerous wall-climbing robots have been developed for these purposes. Most of the climbing robots in literature are large and are intended for maintenance and inspection purposes. Legged structures with two to eight limbs are predominant. Typically, more than two legs provide redundant support and often increase load capacity and safety. However, these benefits are achieved at the cost of increased complexity, size, and weight.

For small robots, however, limited ability to grasp the climbing surface restricts the system to be much more lightweight. In the case of miniature climbing robots, size is limited by the capability of the foot, which for suction is typically in the range of 590gr 80mm from the surface and 365 grams 120 mm from the surface for a 45mm

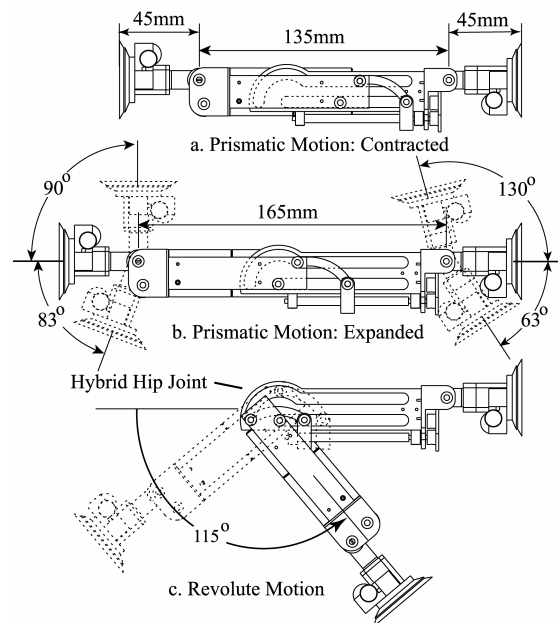


Figure 1. Hybrid hip motion.

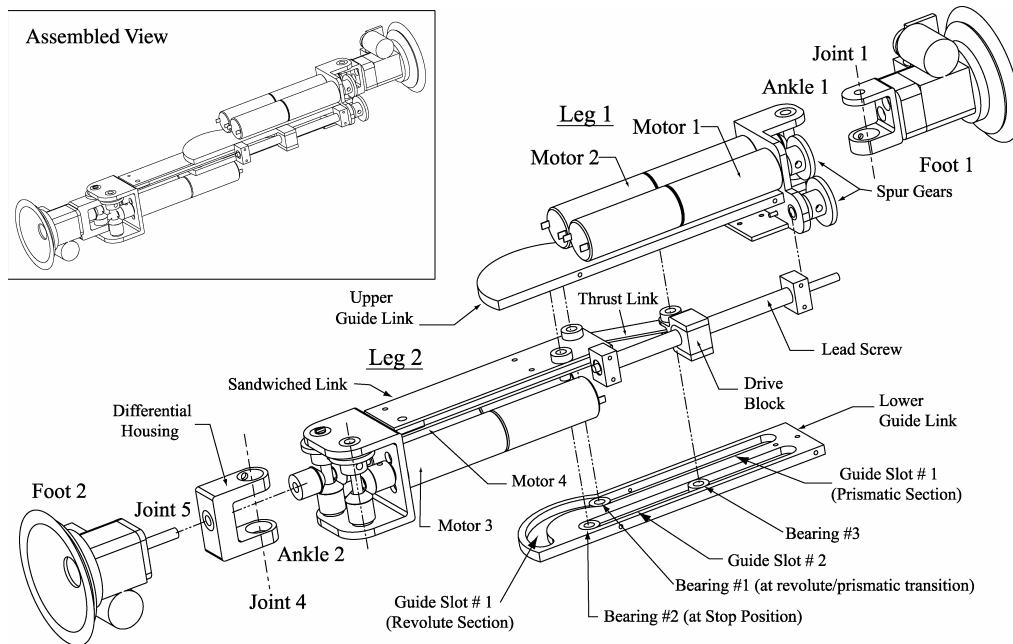


Figure 2. Exploded view of the hybrid hip robot.

suction cup [3]. When fully contracted, the hybrid hip robot presented here measures 50mm by 225mm by 50mm and weighs about 420 grams. Since actuators account for a significant portion of robot weight, their numbers are limited and the challenge is to provide adaptability to surmount a variety of obstacles with limited resources. Hence, the biped is the most common platform since it requires a minimum number of joints and actuators to provide locomotion. Most biped robots use similar ankle structures where articulation is provided to both feet and steering to at least one foot.

Bipeds vary most appreciably in the style of their middle joints: revolute, prismatic or a simple rigid body with no joint at all. Robots using a revolute middle joint include RAMR1 [4], Inchworm [5], Nishi [6], and the robot ROBIN [7]. A prismatic middle joint is used by RAMR2 [8], ROSTAM I-IV [9], and the robot by Yano [10]. Each format of middle joint is predisposed to particular walking and climbing strides that directly influence the mobility of the robot and determine its space requirements. The revolute hip, for example, is well suited to crossing between inclined surfaces and traveling at rapid pace, but it inherently requires a relatively large space for its locomotion. RAMR1 is an example of such a robot in that it moves by anchoring one foot on the surface and then flipping its entire body about that foot. The robot Inchworm requires comparatively less space in that it moves in a crawling stride where one foot is lifted and advanced, which is followed by robot contraction. Due to the revolute hip joint, though, appreciable space is still required for locomotion [5]. In contrast, the prismatic hip

has the potential to crawl through more confined locations. Using a crawling stride similar to Inchworm, RAMR2 is adapted to traveling through confined locations, but is less capable of crossing between surfaces with relative inclination [8].

The robot presented here possesses a hybrid hip joint intended to provide both prismatic and revolute operation, discretely, with a single actuator. It is intended that the hybrid hip robot can travel between surfaces with large relative inclinations as well as through confined spaces. In similar spirit, RAMR1 uses underactuation to couple multiple joints to a single actuator for increased mobility [4, 11, 12]. More similarly, though, RAMR2 [8, 11] drives multiple joints discretely in order to allow a single actuator to drive several revolute or prismatic joints independently. The robot presented here appears to be the first to allow a single actuator to drive a multifunction joint for both revolute and prismatic motion.

3. MECHANICAL STRUCTURE DESIGN

The partially exploded diagram of the hybrid hip robot and an assembled view (inset) are shown in Figure 2. The robot consists of two legs coupled by the hybrid hip joint. Each leg supports an ankle and suction foot for gripping the climbing surface.

A. Legs and Hybrid hip

The two legs of the biped are supported using a specially designed hybrid hip capable of both prismatic and revolute motion, Figure 2. Leg #2 of the robot consists of a link that is sandwiched between the Upper and Lower

Guide Links. The Upper and Lower Guide Links constitute Leg #1 and provide guide slots by which the travel of the sandwiched link is constrained. Friction is minimized by supporting the sandwiched link with roller bearings that run in the slots. Backlash from these slots has been found to be very minimal due to tight tolerances.

Guide slot #1 is designed such that it has a straight section that provides prismatic motion of Leg #2, and a curved section that provides revolute motion. Bearing #1 runs in Guide Slot #1 and is coupled via the Thrust Link to Bearing #3 and the Drive Block. Bearings #2 and #3 run in Guide Slot #2. Power is transmitted from Motor #1 through spur gearing that propels the lead screw and causes the Drive Block to translate linearly. While Bearing #1 is in the Prismatic Section of Guide Slot #1, the entire linkage translates in unison until Bearing #2 reaches the Stop Position, shown in Figure 2. At this instance, Bearing #2 is forced to stop and the Drive Block continues to push Bearing #1 into the Revolute Section of Guide Slot #1. This results in Leg #2 rotating about the axis of Bearing #2 at the Stop Position. When Motor #1 is reversed, the motion of Leg #2 continues in a similar discrete transition between revolute and prismatic motion. Net revolute motion of the hybrid joint is approximately 115°, which is indicated in Figure 1 (c). Net range of prismatic motion is 30mm as indicated between its extreme limits in Figure 1 (a) and (b).

B. Ankle Articulation and Steering

Articulation of the ankles is powered by Motors 2 and 3 via Joints 1 and 4, respectively. The articulation at each end of the legs allows the robot to walk between surfaces with varying inclination. The range of ankle articulation is constrained by the interference between legs and feet as shown in Figure 1 (b). Net range of articulation at Ankle 1 and Ankle 2 is approximately 190° and 200° respectively, as illustrated in. The foot at the end of the sandwiched link has steering capability, which is powered by Motor 4 through a differential housing via Joint 5. Due to differential housing steering of approximately 360° can be attained.

4. HYBRID JOINT OPTIMIZATION

The hybrid hip joint allows discrete prismatic and revolute motion powered by a single actuator. The parameters governing the range of prismatic and revolute motion are the radius of the revolute joint (r), the length of thrust link (L) and the offset distance between the guide slots (d), Figure 3. These three parameters are found such as to minimize the force on the drive block, maximize the prismatic step length, and to obtain revolute angle ($\theta - \theta_0$) up to $2\pi/3$ radians. The initial start angle of rotation is determined by,

$$\theta_0 = \sin^{-1}\left(\frac{d}{r}\right) \quad (1)$$

and the range of prismatic motion is given by,

$$L_p = L_t - \left(\sqrt{L^2 - d^2} + \sqrt{L^2 - r^2}\right) \quad (2)$$

where L_t is the permitted center-to-center length of the Guide Slot #2. Thrust force, which is axial force on the thrust link, F_L and the Drive force, F_D of the link are determined by,

$$F_L = \frac{(P \cos(\theta - \theta_0) - Q r \cos(\theta))g}{r \sin(\theta + \phi)} \quad (3)$$

$$F_D = F_L (\mu \sin(\phi) + \cos(\phi)) \quad (4)$$

where P is maximum torque applied at the hip of the robot. In this case, P was determined by the load of the robot cantilevered from a vertical surface. Q is the total mass of the robot supported by the hip joint; g is acceleration due to gravity and μ is the coefficient of friction. While P and Q are ultimately proportional to robot mass, this quantity was not known at the time of the optimization and these variables were left in their general form to allow iterative consideration of optimization results.

Equations (1) through (4) illustrate the effect of parameters r , L and d on the prismatic length of the joint, L_p , and the forces on the thrust link and drive block. Figure 4 shows the 3-D plots indicating the relationship between the drive force, F_D and the parameter r over the desired range of revolute motion, $\theta_0 \leq \theta \leq 2\pi/3$. It can be concluded from the plots and the equations that for F_D to be minimum, L should be large and θ_0 should be small. In contrast, for L_p to be larger, L should be small and θ_0 should be large. The problem can be expressed as a formal optimization statement where the objective is to find $X = \{r \ L \ d\}$ that,

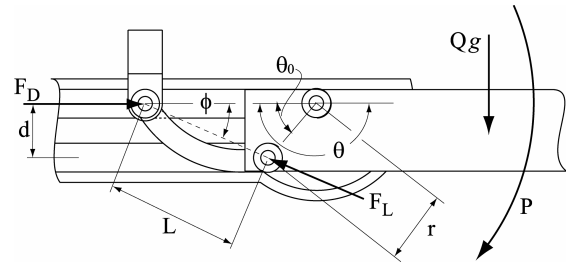


Figure 3: Parameters of the hybrid link

5. KINEMATIC MODEL

A. Coordinate Frames Assignment

Based on the structure of the robot it requires that at least one foot remain in contact with the surface all times. Since the robot is unsymmetrical, it is necessary to consider kinematics and dynamics in two different phases. The coordinate frames are assigned in the three-dimensional space as Left-Foot Supporting (LFS) phase and Right-Foot Supporting (RFS) phase. In the LFS phase the base, coordinate frame is attached to the left foot, which is anchored on the surface. The right foot can move freely with “hand-coordinate frame” attached and vice versa in case of RFS phase. The Figure 7 shows LFS and RFS phases respectively. Modified convention of Denavit-Hartenberg notation is used for defining the link parameters [13]. Tables 1 and 2 shows the link coordinate parameters in LFS and RFS phases respectively.

Note that in the LFS phase, Table 2, $\theta_1, d_2, \theta_3, \theta_4$ and θ_5 are joint variables and a_1, d_2, a_3, d_4 are fixed link parameters. If $d_2 \leq d_{2max}$ then $\theta_3 = \theta_{3min}$ and if $d_2 = d_{2max}$ then $\theta_{3min} \leq \theta_3 \leq \theta_{3max}$. Similarly, in the RFS $\theta_1, \theta_2, \theta_3, d_4$ and θ_5 are joint variables and a_2, d_3, d_4 and a_4 are fixed link parameters. If $d_4 < d_{4max}$ then $\theta_3 = \theta_{3min}$ and if $d_4 = d_{4max}$ then $\theta_{3min} \leq \theta_3 \leq \theta_{3max}$.

B. Forward Kinematics

The final robot transformation matrix can be written as:

$${}^5_0T = \begin{bmatrix} n & s & a & p \\ 0 & 0 & 0 & 1 \end{bmatrix} = \begin{bmatrix} n_x & s_x & a_x & p_x \\ n_y & s_y & a_y & p_y \\ n_z & s_z & a_z & p_z \\ 0 & 0 & 0 & 1 \end{bmatrix} \quad (5)$$

In the LFS phase, the forward kinematics of the robot is derived in the equation sets (6) as follows:

$$\begin{aligned} n_x &= T(1,1) = C_5 C_{134} ; s_x = T(1,2) = -S_5 C_{134} \\ a_x &= T(1,3) = S_{134} \\ p_x &= T(1,4) = a_3 C_{13} + a_1 C_1 + d_2 S_1 \\ n_y &= T(2,1) = C_5 S_{134} ; s_y = T(2,2) = -S_5 S_{134} \\ a_y &= T(2,3) = -C_{134} \\ p_y &= T(2,4) = a_3 S_{13} + a_1 S_1 - d_2 C_1 \\ n_z &= T(3,1) = -S_{235} ; s_z = T(3,2) = -C_{235} \\ a_z &= T(3,3) = 0 ; p_z = T(3,4) = -d_4 \end{aligned} \quad (6)$$

In the RFS phase, the forward kinematics of the robot is obtained in the equation sets (7) as follows:

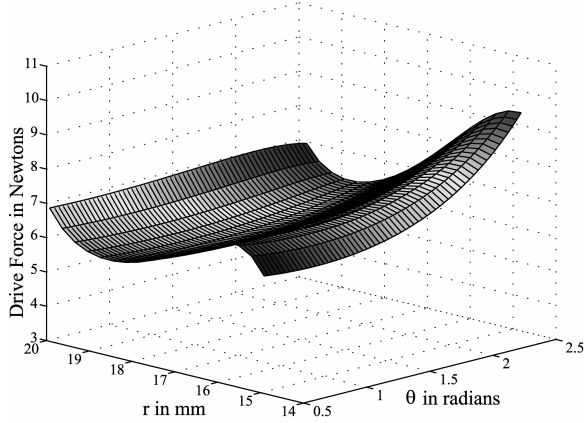


Figure 4: Effect of r and theta on Drive force

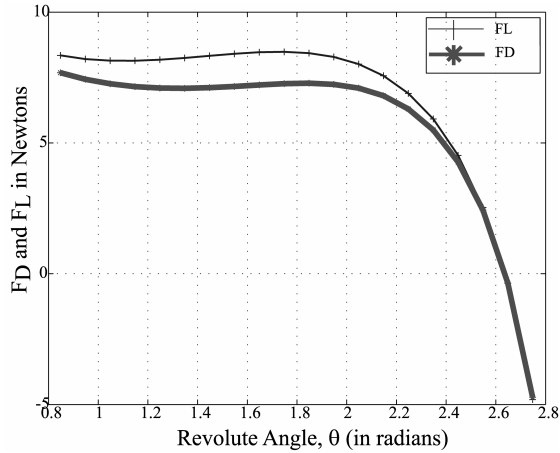


Figure 5: Thrust Link Force and Drive force for optimized parameters, $r = 16, L = 30, d = 12$.

$$\min f(X) = \alpha_1 |F_D| + \alpha_2 \left| \frac{1}{L_p} \right|$$

where $F_D = f(X, \theta)$, $L_p = f(X)$ and α_1 and α_2 are weighting factors

A Matlab line search optimization routine was used with multiple weighting factors, α_1 and α_2 , to determine the best compromise. Ultimately, these weights were selected to be 1.0 and 0.5, respectively, and the optimized values for r, L and d were obtained to be 16mm, 30mm and 12mm, correspondingly. This produced the forces F_D and F_L along the revolute motion, Figure 5, for the optimized parameters r, L and d . The resulting prismatic joint motion was determined to be 30mm.

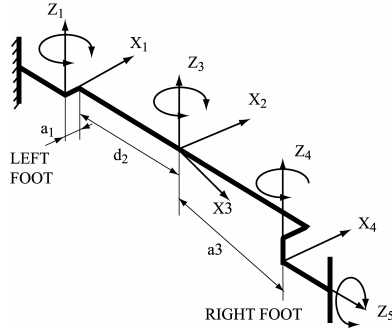


Figure 7: LFS: Coordinate frames

Table 1: Link DH parameters: RFS

i	α_{i-1}	a_{i-1}	d_i	θ_i
1	0	0	0	θ_1
2	$\frac{\pi}{2}$	0	0	θ_2
3	0	a_2	d_3	θ_3
4	$\frac{\pi}{2}$	0	d_4	0
5	$-\frac{\pi}{2}$	a_4	0	θ_5

Table 2: Link DH parameters: LFS

i	α_{i-1}	a_{i-1}	d_i	θ_i
1	0	0	0	θ_1
2	$\frac{\pi}{2}$	a_1	d_2	0
3	$-\frac{\pi}{2}$	0	0	θ_3
4	0	a_3	$-d_4$	θ_4
5	$\frac{\pi}{2}$	0	0	θ_5

$$\begin{aligned}
 n_x &= T(1,1) = C_1 C_{235} ; s_x = T(1,2) = -C_1 S_{235} \\
 a_x &= T(1,3) = S_1 \\
 p_x &= T(1,4) = a_4 C_1 C_{23} + d_4 C_1 S_{23} + a_2 C_1 C_2 + d_3 S_1 \\
 n_y &= T(2,1) = S_1 C_{235} ; s_y = T(2,2) = -S_1 S_{235} \\
 a_y &= T(2,3) = -C_1 \\
 p_y &= T(2,4) = a_4 S_1 C_{23} + d_4 S_1 S_{23} + a_2 S_1 C_2 - d_3 C_1 \\
 n_z &= T(3,1) = S_{235} ; s_z = T(3,2) = C_{235} \\
 a_z &= T(3,3) = 0 \\
 p_z &= T(3,4) = a_4 S_{23} - d_4 C_{23} + a_2 S_2
 \end{aligned} \quad (7)$$

C. Inverse Kinematics

Given a desired foot location, the LFS Inverse Kinematics are thus determined by,

$$\begin{aligned}
 \theta_1 &= \frac{\pi}{2} + \arctan(n_y/n_x) - \arctan(\pm\sqrt{1-x^2}/x) \\
 d_2 &= a_3 \sin(\theta_3) - \cos(\varphi - \theta_1), \theta_3 = \arctan(\pm\sqrt{1-y^2}/y) \\
 \theta_4 &= \arctan(a_x/(-a_y)) - \theta_1 - \theta_3, \theta_5 = \arctan(n_z/s_z) \\
 \text{where : } x &= \frac{a_y s_z}{\sqrt{n_x^2 + n_y^2}}, y = \frac{\cos(\varphi - \theta_1) - a_1}{a_3} \\
 \text{and } \varphi &= \arctan(p_y/p_x)
 \end{aligned}$$

where RFS Inverse Kinematics are determined similarly. The inverse kinematics obtained here are used for motion planning of the robot and will be implemented later in the control algorithm of the robot.

6. WORKSPACE ANALYSIS

The workspace analysis is considered in both LFS and RFS phases. The reachable workspace for LFS phase with

Table 3: LFS workspace data.

Joint Phase	Area (mm ²)
Hybrid hip prismatic only	65712
Hybrid hip revolute only	83542
Complete workspace of the robot with both prismatic and revolute motions	91781

hybrid revolute hip joint and hybrid prismatic hip joint is illustrated in the Figure 6. The exclusive areas swept by the robot with different hybrid hip joint phases are listed in Table 3. The robot can reach an area of 65712 mm² and 83542 mm² when the hybrid joint is in prismatic and revolute motions, respectively. The cumulative workspace is thus 91781 mm², which is 40% larger than the prismatic space and 10% greater than the revolute space. The robot passing through confined and inclined environments is shown in Figure 8 and Figure 9 respectively.

7. CONCLUSIONS

A new hybrid hip joint designed for improving adaptability of miniature climbing robots in various environments is presented. The joint is optimized relative to the robot size, weight and actuation. The kinematics and workspace of the entire robot with hybrid hip are analyzed. The calculations show a promising increase in reachable workspace with the addition of revolute motion,

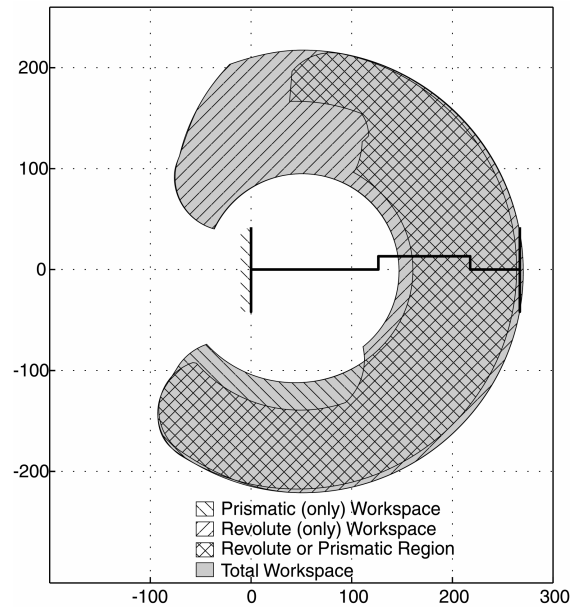


Figure 6. LFS Workspace diagram.

which should improve performance of the robot in both, confined and inclined environments. Future work will focus on motion planning and experimental testing of the robot.

8. REFERENCES

1. Nunobiki, M., M. Hasegawa, K. Okuda, N. Huruse, and Y. Takita, "Study on the gaits of an inchworm robot through a narrow path," *Advanced Robotics*, 13(3), p329-30, 1999.
2. Briones, L., P. Bustamante, and M. Serna, "Robicen: A wall climbing pneumatic robot for inspection in nuclear power plants," *Robotics & Computer-Integrated Manufacturing*, 11(4), p287-292, 1994.
3. Dangi, G., J. Stam, and D. Aslam, "Design, Fabrication, and Testing of a Smart Robotic Foot for Microrobotic Systems", *Proceedings of the 31st International Symposium on Robotics (ISR 2000)*, Montreal, Que., Canada, p283-287, 2000.
4. Minor, M., H. Dulimarta, G. Danghi, R. Mukherjee, R. Lal Tummala, and D. Aslam, "Design, implementation, and evaluation of an under-actuated miniature biped climbing robot", *Proceedings. 2000 IEEE/RSJ International Conference on Intelligent Robots and Systems (IROS 2000)*, Piscataway, NJ, USA, p1999-2005 vol.3, 2000.
5. Kotay, K.D. and D.L. Rus, "Navigating 3D steel web structures with an inchworm robot", *Proceedings of IEEE/RSJ International Conference on Intelligent Robots and Systems. IROS '96*, New York, NY, USA, p368-75 vol.1, 1996.
6. Nishi, A., "Development of Wall Climbing Robots," *Computers & Electrical Engineering*, 22(2), p123-149, 1996.
7. Pack, R.T., J.L. Christopher, and K. Kawamura, "A Rubbertuator-Based Structure-Climbing Inspection Robot", *Proceedings of the 1997 IEEE International Conference on Robotics and Automation, ICRA.*, Albuquerque, NM., 3, p1869-74, 1997.
8. Xiao, J., M. Minor, H. Dulimarta, N. Xi, R. Mukherjee, and R.L. Tummala, "Modeling and control of an under-actuated miniature crawler robot", *Proceedings of RSJ/IEEE International Conference on Intelligent Robots and Systems*, Piscataway, NJ, USA, p1546-51 vol.3, 2001.
9. Bahr, B., Y. Li, and M. Najafi, "Design and Suction Cup Analysis of a Wall Climbing Robot," *Computers & Electrical Engineering*, 22(3), p193-209, 1996.
10. Yano, T., T. Suwa, M. Murakami, and T. Yamamoto, "Development of a Semi Self-Contained Wall Climbing Robot with Scanning Type Suction Cups", *Proceedings of the 1997 IEEE/RSJ International Conference on Intelligent Robot and Systems*, Grenoble, Fr., 2, p900-905, 1997.

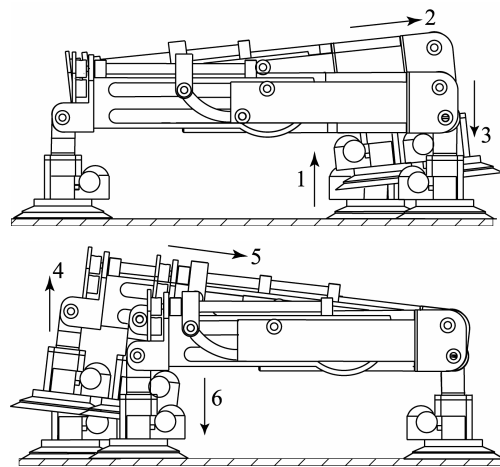


Figure 8. Robot in confined space

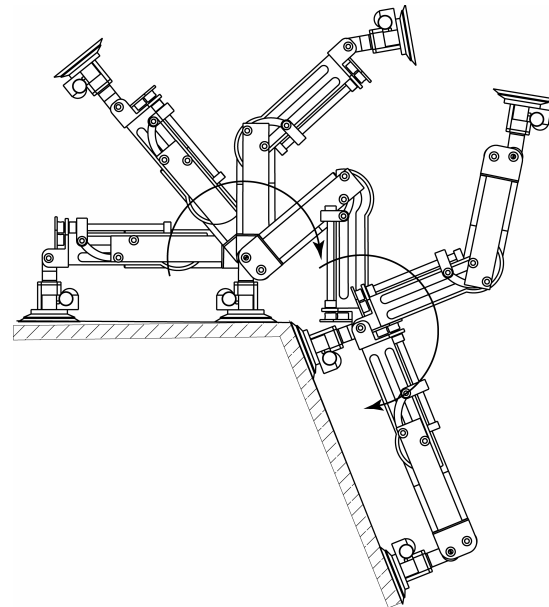


Figure 9. Robot passing between inclined surfaces

11. Minor, M. and R. Mukherjee, "Under-Actuated Kinematic Structures for Miniature Climbing Robots," *ASME Journal of Mechanical Design*, accepted with minor revisions, 2002.
12. Yue, M., N. Xi, M. Minor, and R. Mukherjee, "Dynamic workspace analysis and motion planning for a micro biped walking robot", *Proceedings. 2000 IEEE/RSJ International Conference on Intelligent Robots and Systems (IROS 2000)*, Piscataway, NJ, USA, p1900-5 vol.3, 2000.
13. Craig, J.J., *Introduction to Robotics: Mechanics and Control*, Reading, MA: Addison Wesley Publishing Co., 1986.